Entropically Driven Enhancement of Cleavage Activity of a DNA-Armed Hammerhead Ribozyme: Mechanism of Action of Hammerhead Ribozymes

Masaki Warashina,[†,‡,§] Yasuomi Takagi,[‡,§] Shinya Sawata,[‡,§] De-Min Zhou,[†,‡,§] Tomoko Kuwabara,[†,‡,§] and Kazunari Taira*[,†,‡,§]

National Institute for Advanced Interdisciplinary Research, and National Institute of Bioscience and Human Technology, Agency of Industrial Science & Technology, MITI, Tsukuba Science City 305, Japan, and Institute of Applied Biochemistry, University of Tsukuba, Tennoudai 1-1-1, Tsukuba Science City 305, Japan

Received July 9, 1997[⊗]

Recent X-ray structures of hammerhead ribozymes demanded rearrangement of the scissile phosphate backbone into a conformation suitable for in-line attack by the 2′-oxygen in the transition state or prior to it. As part of our efforts to detect the putative conformational change and also to characterize the transition state structure of a hammerhead ribozyme-catalyzed reaction, kinetic and thermodynamic parameters of a chimeric RNA/DNA ribozyme were compared with the corresponding values of an all-RNA ribozyme. Kinetic analysis revealed that (i) DNA portions enhanced k_{cat} in the entire pH region between 6 and 9, and at all temperatures between 0 and 60 °C; (ii) the origin of the acceleration in k_{cat} by the chimeric DNA-armed ribozyme was accomplished by two distinctly different phenomena: at the temperatures below 25 °C, the enhancement originated from the acceleration of dissociation of the products from the reaction complex (k_{diss}), whereas at temperatures 25−45 °C, the DNA-portions enhanced the chemical cleavage (k_{cleav}) of the ribozyme-catalyzed reaction; (iii) under any reaction conditions used in this study, a conformational change in the ribozyme·substrate complex did not become the rate-limiting step; and (iv) importantly, the enhancement of cleavage activity by the chimeric DNA-armed ribozyme was driven entropically, a result that cannot simply be explained by the recently proposed "fraying model" with open and closed ribozyme·substrate helixes (Hertel et al. *Proc. Natl. Acad. Sci. U.S.A.* **1997**, *94*, 8497−8502).

Introduction

Hammerhead-type ribozymes are RNA enzymes that act in cis in nature[1] but have also been engineered such that they act in trans (Figure 1).[2,3] Their potential as therapeutic agents has been demonstrated.[4,5] To elucidate structure−function relationships and to improve their exogenous therapeutic application, several mixed RNA/DNA ribozymes and other modified ribozymes have been synthesized chemically.[6−14] Examination of the mixed RNA/DNA ribozymes revealed that most deoxyribonucleotide substitutions can be tolerated. However, in the majority of cases, catalytic activities are somewhat reduced.[6,8] When the rate-limiting step is the product-release step (k_{diss}, Figure 2), modifications that lower the affinity for substrate (and, thus, for product as well) enhance the catalytic activity. In fact, the first example of such an acceleration has been demonstrated for *Tetrahymena* ribozyme; the rate-limiting step in the

* To whom correspondence should be addressed, as follows: Professor Kazunari Taira, Institute of Applied Biochemistry, University of Tsukuba, 1-1-1 Tennoudai, Tsukuba Science City 305, Japan. Phone: 81(Japan)-298-53-4623. Fax: 81(Japan)-298-53-4623. E-mail: taira@nibh.go.jp.

† National Institute for Advanced Interdisciplinary Research.

‡ National Institute of Bioscience and Human Technology.

§ Institute of Applied Biochemistry.

⊗ Abstract published in *Advance ACS Abstracts,* November 15, 1997.

(1) Symons, R. H. *Trends Biochem. Sci.* **1989**, *14*, 445−450.

(2) Uhlenbeck, O. C. *Nature* **1987**, *328*, 596−600.

(3) Haseloff, J.; Gerlach, W. L. *Nature* **1988**, *334*, 585−591.

(4) Sarver, N.; Cantin, E.; Chang, P.; Ladne, P.; Stephens, D.; Zaia, J.; Rossi, J. *Science* **1990**, *247*, 1222−1225.

(5) Marschall, P.; Thompson, J. B.; Eckstein, F. *Cell. Mol. Neurobiol.* **1994**, *14*, 523−538.

(6) (a) Perreault, J.-P.; Wu, T.-F.; Cousineau, B.; Ogilvie, K. K.; Cedergren, R. *Nature* **1990**, *344*, 565−567. (b) Perreault, J.-P.; Labuda, D.; Usman, N.; Yang, J.-H.; Cedergren, R. *Biochemistry* **1991**, *30*, 4020−4025. (c) Yang, J.-H.; Perreault, J.-P.; Labuda, D.; Usman, N.; Cedergren, R. *Biochemistry* **1990**, *29*, 11156−11160. (d) Chartrand, P.; Harvey, S. C.; Ferbeyre, G.; Usman, N.; Cedergren, R. *Nucleic Acids Res.* **1995**, *23*, 4092−4096.

(7) (a) Taira, K.; Nishikawa, S. In *Gene Regulation, Biology of Antisense RNA and DNA*; Erickson, R. P., Izant, J. G., Eds.; Raven Press: New York, 1992; pp 35−54. (b) Shimayama, T.; Sawata, S.; Komiyama, M.; Takagi, Y.; Tanaka, Y.; Wada, A.; Sugimoto, N.; Rossi, J. J.; Nishikawa, F.; Nishikawa, S.; Taira, K. *Nucleic Acids Res. Symp. Ser.* **1992**, *27*, 17−18. (c) Shimayama, T.; Nishikawa, F.; Nishikawa, S.; Taira, K. *Nucleic Acids Res.* **1993**, *21*, 2605−2611. (d) Sawata, S.; Shimayama, T.; Komiyama, M.; Kumar, P. K. R.; Nishikawa, S.; Taira, K. *Nucleic Acids Res.* **1993**, *21*, 5656−5660. (e) Shimayama, T. *Gene* **1994**, *149*, 41−46. (f) Shimayama, T.; Nishikawa, S.; Taira, K. *FEBS Lett.* **1995**, *368*, 304−306. (g) Wada, A.; Shimayama, T.; Zhou, D.-M.; Warashina, M.; Orita, M.; Koguma, T.; Ohkawa, J.; Taira, K. In *Controlled Drug Delivery: Challenges and Strategies*; Park, K., Ed.; ACS Professional Reference Book; American Chemical Society: Washington, DC, 1997; pp 357−385.

(8) (a) Pieken, W. A.; Olsen, D. B.; Benseler, F.; Aurup, H.; Eckstein, F. *Science* **1991**, *253*, 314−317. (b) Olsen, D. B.; Benseler, F.; Aurup, H.; Pieken, W. A.; Eckstein, F. *Biochemistry* **1991**, *30*, 9735−9741. (c) Williams, D. M.; Pieken, W. A.; Eckstein, F. *Proc. Natl. Acad. Sci. U.S.A.* **1992**, *89*, 918−921. (d) Tuschl, T.; Eckstein, F. *Proc. Natl. Acad. Sci. U.S.A.* **1993**, *90*, 6991−6994. (e) Tuschl, T.; Ng, M. M. P.; Pieken, W.; Benseler, F.; Eckstein, F. *Biochemistry* **1993**, *32*, 11658−11668. (f) Ng, M. M. P.; Benseler, F.; Tuschl, T.; Eckstein, F. *Biochemistry* **1994**, *33*, 12119−12126. (g) Heidenreich, O.; Benseler, F.; Fahrenholz, A.; Eckstein, F. *J. Biol. Chem.* **1994**, *269*, 2131−2138.

(9) (a) McCall, M. J.; Hendry, P.; Jennings, P. A. *Proc. Natl. Acad. Sci. U.S.A.* **1992**, *89*, 5710−5714. (b) Hendry, P.; McCall, M. J.; Santiago, F. S.; Jennings, P. A. *Nucleic Acids Res.* **1992**, *20*, 5737−5741. (c) Hendry, P.; McCall, M. J. *Nucleic Acids Res.* **1995**, *23*, 3928−3936. (d) Hendry, P.; McCall, M. J. *Nucleic Acids Res.* **1996**, *24*, 2679−2684.

(10) Taylor, N. R.; Kaplan, B. E.; Swiderski, P.; Li, H.; Rossi, J. J. *Nucleic Acids Res.* **1992**, *20*, 4559−4565.

(11) (a) Fu, D.-J.; McLaughlin, W. *Proc. Natl. Acad. Sci. U.S.A.* **1992**, *89*, 3985−3989. (b) Fu, D.-J.; McLaughlin, L. W. *Biochemistry* **1992**, *31*, 10941−10949. (c) Fu, D. J.; Rajur, S. B.; McLaughlin, L. W. *Biochemistry* **1993**, *32*, 10629−10637. (d) Bevers, S.; Xiang, G. B.; Mclaughlin, L. W. *Biochemistry* **1996**, *35*, 6483−6490.

S0022-3263(97)01241-3 CCC: $14.00

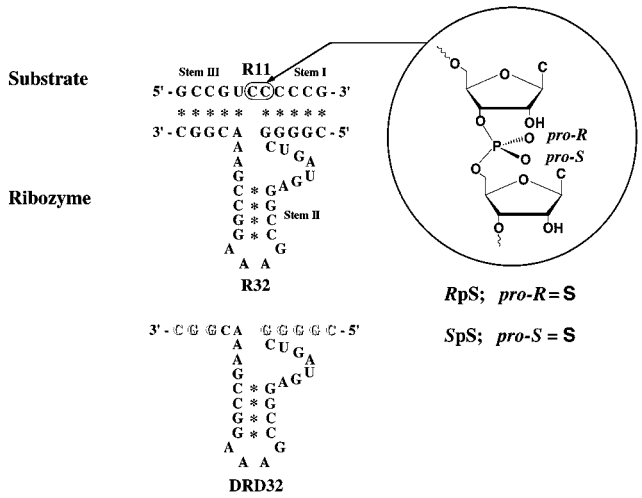

Figure 1. Structures of all-RNA (R32) and chimeric DNA/RNA (DRD32) ribozymes and a substrate (R11). RNA and DNA regions are indicated by bold and outlined letters, respectively. The substrate-binding regions (stems I and III) are short to avoid the rate-limiting product-dissociation step (Figure 2; k_{diss}). Also, the binding sequence was designed so that self-complementations and intersubstrate complementations could be avoided. An expanded view of the cleavage site is also shown within the circle to provide details of the phosphodiester linkage in the unmodified substrate (R11). In the case of modified substrate with a phosphorothioate linkage, either *pro-R*p or *pro-S*p of a nonbridging phosphoryl oxygen is replaced by a sulfur atom at the cleavage site of the R11 substrate to yield epimers named *R*pS and *S*pS, respectively.

reaction catalyzed by the *Tetrahymena* ribozyme is the product-release step since replacement of one of the phosphoryl oxygens at the cleavage site by sulfur, which slows down the cleavage reaction, has little effect on the overall rate of the reaction (no "thio-effect" is apparent in this case).[15,16] Therefore, Cech's group successfully improved the activity of *Tetrahymena* ribozyme by mutating nonconserved sequences with resultant decreased affinity for RNA and, thus, higher turnover.[17] However, mutations that increased the turnover number were associated with a slower chemical-cleavage step. Enhancement in k_{cat} is also reported for hammerhead ribozymes.[7,9,10] The enhancement in k_{cat} was accomplished by the introduction of DNA at the substrate-binding sites (stems I and III). The origin of the acceleration was based on two distinctly different phenomena: (i) in case of the study by Rossi's group, the enhancement originated from the acceleration of dissociation of the products from the reaction complex (k_{diss}; Figure 2)[10] and (ii) in case of the study by Hendry et al., the rate-limiting step for the chimeric DNA/RNA ribozyme was the chemical-cleavage step (k_{cleav}), although, for their all-RNA ribozyme, the rate-limiting step appeared still to be the product-dissociation step.[9b]

As compared to that of the *Tetrahymena* ribozyme,[17] the chemical step of the reaction catalyzed by hammerhead-type ribozymes is about 2 orders of magnitude slower,[18] and thus, it can potentially be the rate-limiting step. In fact, Uhlenbeck and others have demonstrated a thio effect for hammerhead ribozymes,[19] and Uhlenbeck's and Herschlag's groups also elegantly measured individual elementary rate constants for substrate-binding, cleavage, and product-release steps and demonstrated a change of the rate-limiting step depending on the length of the substrate.[20] Since we are interested in structure−function relationships of chimeric RNA/DNA ribozymes, we tried, in designing the ribozymes, to minimize the substrate-binding sequence and, thereby, to increase the rate of the product-release step (Figures 1 and 2).[7,21−25] Then, ambiguity regarding the rate-limiting step should be minimized.

Recently, two independent groups have reported three-dimensional pictures of the hammerhead ribozyme.[26,27] McKay's group used a DNA substrate whereas Scott and Klug used a natural RNA substrate except at the cleavage site. Despite the difference in the components of the substrates, the overall fold of the structure was nearly identical, stems II and III were collinear to yield an overall γ-shape structure. However, both crystal structures were not in a conformation that would support an "in-line" mechanism of RNA strand cleavage.[19] Therefore, the ground-state X-ray structure is expected to undergo a conformational change in the transition state or prior to it. Such a conformational intermediate was captured by freeze-trapping the RNA prior to cleavage.[27c] However, the newly captured conformational intermediate appears to require further conformational change in order to facilitate the following *in-line* attack. We recently presented evidence for the absence of a kinetic isotope effect in hammerhead ribozyme phosphodiester cleavage, indicating the nonexistence of a proton-transfer process in the rate-limiting step of the cleavage reaction.[21]

(12) Dahm, S. C.; Uhlenbeck, O. C. *Biochchimie* **1990**, *72*, 819−823.
(13) (a) Adams, C. J.; Murray, J. B.; Farrow, M. A.; Arnold, J. R. P.; Stockley, P. G. *Tetrahedron Lett.* **1995**, *36*, 5421−5424. (b) Murray, J. B.; Adams, C. J.; Arnold, J. R. P.; Stockley, P. *Biochem. J.* **1995**, *311*, 487−494. (c) Hendrix, C.; Mahieu, M.; Anne, J.; Vancalenbergh, S.; Vanaerschot, A.; Content, J.; Herdewijn, P. *Biochem. Biophys. Res. Commun.* **1995**, *210*, 67−73. (d) Tanaka, H.; Endo, T.; Hosaka, H.; Takai, K.; Yokoyama, S.; Takaku, H. *Bioorg. Med. Chem. Lett.* **1994**, *4*, 2857−2862. (e) Heidenreich, O.; Xu, X.; Swiderski, P.; Rossi, J.; Nerenberg, M. *Antisense Nucleic Acid Drug Dev.* **1996**, *6*, 111−118.
(14) (a) Beigelman, L.; Karpeisky, A.; Matulicadamic, J.; Haeberli, P.; Sweedler D.; Usman, N. *Nucleic Acids Res.* **1995**, *23*, 4434−4442. (b) Usman, N.; Beigelman, L.; Mcswiggen, J. A. *Curr. Opin. Struct. Biol.* **1996**, *6*, 527−533.
(15) McSwiggen, J. A.; Cech, T. R. *Science* **1989**, *244*, 679−683.
(16) Rajagopal, J.; Doudna, J. A.; Szostak, J. W. *Science* **1989**, *244*, 692−694.
(17) Young, B.; Herschlag, D.; Cech, T. R. *Cell* **1991**, *67*, 1007−1019.
(18) Fedor, M. J.; Uhlenbeck, O. C. *Proc. Natl. Acad. Sci. U.S.A.* **1990**, *87*, 1668−1672.
(19) (a) Uhlenbeck, O. C.; Dahm, S. C.; Ruffner, D. E.; Fedor, M. *Nucleic Acids Res. Symp. Ser.* **1989**, *21*, 95−96. (b) van Tol, H.; Buzayan, J. M.; Feldstein, P. A.; Eckstein, F.; Bruening, G. *Nucleic Acids Res.* **1990**, *18*, 1971−1975. (c) Dahm, S. C.; Uhlenbeck, O. C. *Biochemistry* **1991**, *30*, 9464−9469. (d) Koizumi, M.; Ohtsuka, E. *Biochemistry* **1991**, *30*, 5145−5150. (e) Slim, G.; Gait, M. J. *Nucleic Acids Res.* **1991**, *19*, 1183−1188.
(20) (a) Fedor, M. J.; Uhlenbeck, O. C. *Biochemistry* **1992**, *31*, 12042−12054. (b) Hertel, K. J.; Peracchi, A.; Uhlenbeck, O. C.; Herschlag, D. *Proc. Natl. Acad. Sci. U.S.A.* **1997**, *94*, 8497−8502.
(21) (a) Sawata, S.; Komiyama, M.; Taira, K. *J. Am. Chem. Soc.* **1995**, *117*, 2357−2358. (b) Kumar, P. K. R.; Zhou, D.-M.; Yoshinari, K.; Taira, K. In *Catalytic RNA*; Eckstein, F., Lilley, D. M. J., Eds.; Springer: Berlin, 1996; Nucleic Acids and Molecular Biology, Vol. 10; pp 217−230.
(22) Takagi, Y.; Taira, K. *FEBS Lett.* **1995**, *361*, 273−276.
(23) Orita, M.; Vinayak, R.; Andrus, A.; Warashina, M.; Chiba, A.; Kaniwa, H.; Nishikawa, F.; Nishikawa, S.; Taira, K. *J. Biol. Chem.* **1996**, *271*, 9447−9454.
(24) (a) Zhou D.-M.; Usman, N.; Wincott, F. E.; Matulic-Adamic, J.; Orita, M.; Zhang, L.-H.; Komiyama, M.; Kumar, P. K. R.; Taira, K. *J. Am. Chem. Soc.* **1996**, *118*, 5862−5866. (b) Zhou D.-M.; Kumar, P. K. R.; Zhang, L.-H.; Taira, K. *J. Am. Chem. Soc.* **1996**, *118*, 8969−8970.
(25) Uebayasi, M.; Uchimaru, T.; Koguma, T.; Sawata, S.; Shimayama, T.; Taira, K. *J. Org. Chem.* **1994**, *59*, 7414−7420.
(26) (a) Pley, H. W.; Flaherty, K. M.; Mckay, D. B. *Nature* **1994**, *372*, 68−74. (b) Mckay, D. B. *RNA* **1996**, *2*, 395−403.
(27) (a) Scott, W. G.; Finch, J. T.; Klug, A. *Cell* **1995**, *81*, 991−1002. (b) Scott, W. G.; Klug, A. *Trends Biochem. Sci.* **1996**, *21*, 220−224. (c) Scott, W. G.; Murray, J. B.; Arnold, J. R. P.; Stoddard, B. L.; Klug, A. *Science* **1996**, *274*, 2065−2069.

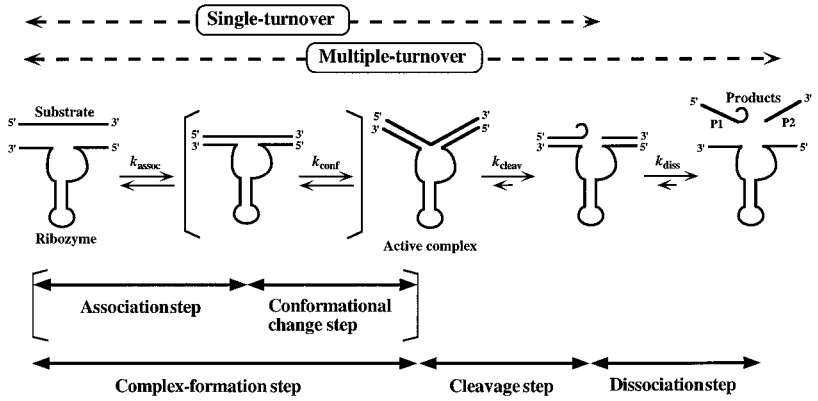

Figure 2. Schematic representation of the kinetics of the ribozyme-catalyzed reaction. The reaction of the hammerhead ribozyme consists of at least three steps. The substrate (and magnesium ions) first bind(s) to the ribozyme (k_{assoc}). The phosphodiester bond of the bound substrate is cleaved by the action of a magnesium ion (k_{cleav}). The cleaved fragments dissociate from the ribozyme, and the liberated ribozyme is now available for a new series of catalytic events (k_{diss}). A conformational change may be required to form an active ribozyme/substrate complex (k_{conf}).

This result was consistent with the interpretation that the 5′-oxygen at the cleavage site is not protonated by a general acid catalyst, but rather is bound directly by a Lewis acid catalyst such as a Mg^{2+} ion, as the nucleophilic 2′-oxygen is bound directly to a Mg^{2+} ion. However, our observation was questioned,[27b] suggesting that in our ribozyme system we might have just observed a rate-limiting conformational change and thus there was no kinetic isotope effect. Indeed, such a rate-limiting conformational change was reported for a ribozyme-catalyzed reaction.[9c]

To clarify this problem we reexamined our system using both a natural all-RNA 32-mer ribozyme (R32) and the corresponding DNA-armed ribozyme (DRD32). Since the rate of chemical cleavage (k_{cat}) by the DRD32 is faster than that by R32,[7] any putative conformational change would be expected to be detectable more easily in the case of the DNA-armed ribozyme. We report herein a comparison of the thermodynamic parameters and kinetic behaviors of an all-RNA and DNA-armed ribozymes and find that both show nearly identical pH and temperature dependencies. This analysis supports the lack of a conformational change in the rate-limiting step for our ribozyme system. Furthermore, we confirmed that DNA components of the binding arms enhanced the chemical cleavage step and that the enhancement was driven entropically.

Materials and Methods

Synthesis of Chimeric DNA/RNA Ribozymes and Substrates. All substrates and ribozymes were chemically synthesized on a DNA synthesizer [394; Applied Biosystems, Division of Perkin-Elmer Co. (ABI), CA]. RNA reagents were purchased either from ABI or Glen Research (VA). Purification of the synthesized oligonucleotides was performed as described in the ABI user bulletin (no. 53; 1989) with minor modifications.[7c] In brief, synthesized oligonucleotides were incubated in 2 mL of concentrated ammonia/ethanol (3:1) at 55 °C for 8 h to remove protecting groups. The supernatant was lyophilized in a Speed-Vac concentrator (Savant, NY) and incubated with 1 M tetrabutylammonium fluoride in THF at room temperature for 15 h to remove 2′-protecting *tert*-butyldimethylsilyl groups. After addition of the same amount of 0.1 M triethylamine acetate, the mixture was lyophilized again. The crude deprotected oligonucleotides were then purified on a fast desalting column, by reverse-phase HPLC, and by electrophoresis on a 20% polyacrylamide/7 M urea denaturing gel with subsequent extraction from the gel with elusion buffer [0.3 M ammonium acetate, 0.1 mM EDTA, 20 mM Tris-HCl (pH 8.0)]. A substrate into which a phosphorothioate linkage was introduced at the cleavage site was also synthesized chemically and two isomers (*R*p and *S*p) were separated by reverse-phase HPLC. The separated *R*p substrate was incubated with a 2-fold excess of ribozyme and 25 mM Mg^{2+} at 37 °C for 1 h, and then it was purified by HPLC again to remove the small amount of contaminating normal and *S*p substrates.[25] The concentration of the purified substrates and ribozymes were determined from their absorption at 260 nm. To make sure that there was the same relative amount of active ribozyme in the all-RNA and chimeric mixtures, all of them were deprotected and purified under the same conditions. Moreover, their purities were confirmed to be the same by ^{32}P-labeling. RNA sequences were determined by sequencing and the positions of DNA components in the chimeric oligonucleotides were determined by alkaline hydrolysis.

Kinetic Measurements. In general, reactions were carried out at 37 °C, in 25 mM $MgCl_2$ and 50 mM Tris-HCl (pH 8.0; except for the pH-rate profile). Reactions were stopped by removing aliquots from the reaction mixture at appropriate intervals and mixing them with an equivalent volume of a solution that contained 100 mM EDTA, 9 M urea, 0.1% xylene cyanol, and 0.1% bromophenol blue. Substrates and 5′-cleaved products were separated by electrophoresis on a 20% polyacrylamide/7 M urea denaturing gel and were detected by autoradiography. The extent of cleavage was determined by quantitation of radioactivity in the bands of substrate and product with a Bio-Image Analyzer (BA100 or BA2000; Fuji Film, Tokyo).

For the kinetic measurements under saturating (k_{cat}) conditions, for which one example of such results is shown in Figure 3A, each fully ^{32}P-labeled ribozyme (R32 or DRD32) in 4 μL of 25 mM $MgCl_2$ and 50 mM Tris-HCl, pH 8.0, was preincubated at 37 °C. Similarly, partially ^{32}P-labeled substrate (R11) in a larger volume was also preincubated at 37 °C. Each reaction was initiated by adding a 1 μL aliquot of substrate to each solution of ribozyme (the final concentrations of substrate and ribozyme were 87 μM and 0.3 μM, respectively). Reactions were stopped by removal of 2.5 μL aliquots from the reaction mixture (R11:R32 or R11:DRD32 combinations) at 10 min (lanes 2 and 5) and 20 min (lanes 3 and 6) and mixing with an equivalent volume of a solution that contained 100 mM EDTA, 9 M urea, 0.1% xylene cyanol, and 0.1% bromophenol blue. The substrate and 5′-cleaved product were separated by electrophoresis on a 20% polyacrylamide/7 M urea denaturing gel and were detected by autoradiography. The extent of cleavage was determined by quantitation of radioactivity in the bands of substrate and product with the Fuji Bio-Image Analyzer BA100 or BA2000.

The reaction conditions for cleavage of the phosphorothioate linkages (Figure 3B) were basically the same as described

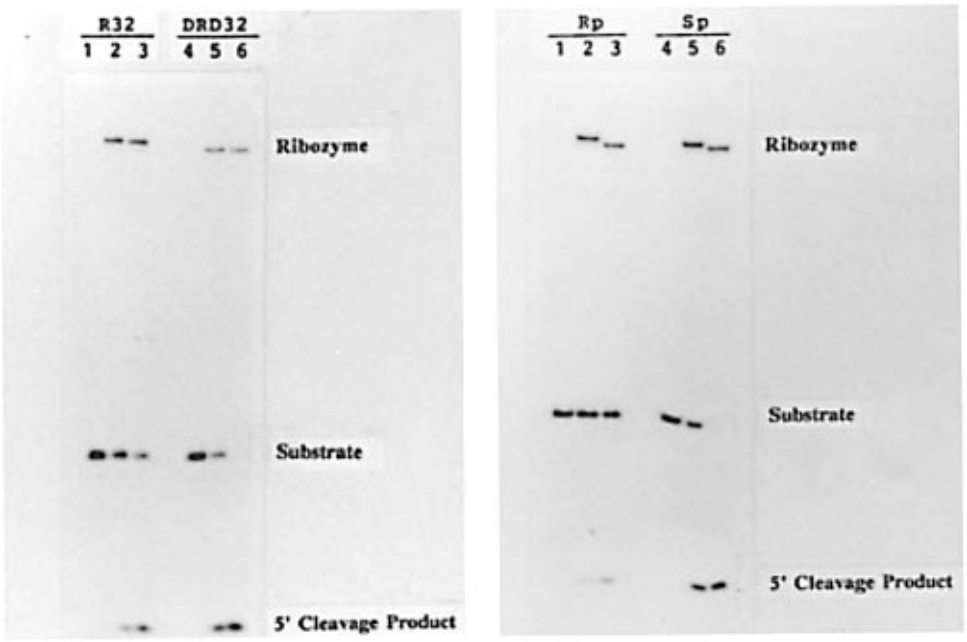

Figure 3. Difference in reactivity between the all-RNA R32 ribozyme and the DNA-armed DRD32 ribozyme.[7g] (A, Left) Reactions of fully ^{32}P-labeled ribozymes and partially ^{32}P-labeled substrates under saturating (k_{cat}) conditions. The ratio of substrate to ribozyme was roughly 300:1. To show both substrate and ribozyme on the same gel, substrate molecules were only partially ^{32}P-(5′)-end-labeled. Lanes 1 and 4 represent labeled substrates (R11) before addition of the ribozymes. To the substrates, either the ^{32}P-labeled all-RNA ribozyme (R32, lanes 2 and 3) or the chimeric DRD32 ribozyme (lanes 5 and 6) was added, and the reaction was monitored 10 min (lanes 2 and 5) and 20 min (lanes 3 and 6) after mixing at 37 °C, in 25 mM $MgCl_2$ and 50 mM Tris-HCl (pH 8.0). Note that the chimeric DRD32 ribozyme has higher cleavage activity than the wild-type all-RNA R32 ribozyme. (B, Right) Cleavage of a modified RNA substrate with one phosphorothioate linkage at the cleavage site (*R*pS or *S*pS). Lanes 1 and 4 are intact thio substrates with the *R*p and *S*p configurations, respectively. To these substrates either the R32 (lanes 2 and 5) or the DRD32 (lanes 3 and 6) ribozyme was added, and mixtures were incubated for 10 min. Both the all-RNA R32 ribozyme and the chimeric DRD32 ribozyme can cleave the *S*p isomer (lanes 5 and 6). The cleavage rate is nearly identical with that for R11. However, the *R*p isomer is much more resistant to the digestion by both R32 and DRD32 ribozymes (lanes 2 and 3). The conditions for the cleavage reactions were basically the same as those described in (A).

above. The concentration of substrates (*R*p or *S*p isomers) was 2 μM and that of the ribozymes (R32 or DRD32) was 0.2 μM. Either R32 (Figure 3B; lanes 2 and 5) or DRD32 (lanes 3 and 6) ribozyme was added to the same amount of the *R*p or *S*p isomer, and reactions were incubated for 10 min. The reactions were stopped and monitored as described above.

The pH−log(k_{cat}) profiles of Figure 4 were obtained similarly under saturating conditions. For the measurements of deuterium isotope effects, all the reagents used were dissolved in D_2O, and evaporation and redissolving procedures were repeated to allow complete exchange of protons.[21] pD was adjusted at 37 °C.

In the Arrhenius plots shown in Figure 6, reaction rates were measured, in 25 mM $MgCl_2$ and 50 mM Tris-HCl (pH 8.0; adjusted at each temperature), either (i) under the ribozyme-saturating (single-turnover) conditions at 0 °C or (ii) under the substrate-saturating (multiple-turnover) conditions over a range of temperatures from 15 to 60 °C. In all cases, kinetic measurements were made under conditions where all the available ribozyme or substrate was expected to form a Michaelis−Menten complex. These conditions were achieved by employing high concentrations of either the ribozyme (<3.8 μM) or the substrate (<1.1 μM).

All kinetic measurements were performed at least in triplicate, and the reported kinetic parameters were the average values in that potential errors were found to be 30% for each measurement.

Results and Discussion

DNA-Arms Enhance the k_{cat} Value. As part of our efforts at elucidating structure−function relationships, we compared the kinetic and thermodynamic features of all-RNA and chimeric DNA-armed ribozymes. Figure 1 shows structures of ribozymes used in this study. R32 is an all-RNA 32-mer ribozyme. DRD32 is a chimeric ribozyme consisting of DNA (stem I), RNA (catalytic loop, stem II and its loop), and DNA (stem III) regions. In our ribozyme system, to avoid kinetic complexities, ribozymes with substrate-binding arms reduced in length (stems I and III) were used.[7,21−25] Recall that when a longer binding sequence is used, the product-dissociation step (k_{diss}) rather than the chemical step (k_{cleav}) becomes the rate-limiting step (Figure 2).[20]

Reactivity difference in R32- and DRD32-catalyzed reactions was examined under substrate-saturating (k_{cat}) conditions (Figure 3A) by the use of fully ^{32}P-labeled ribozymes and partially ^{32}P-labeled substrates. Although the ratio of substrate to ribozyme was roughly 300:1, to show both on the same gel, substrate molecules were only partially ^{32}P-(5′)-end-labeled. Thus, only a small fraction of the substrate was ^{32}P-labeled, and an excess of unlabeled substrate was mixed with the labeled substrate. Therefore, the intensities of the bands (ribozyme vs substrate) do not reflect the actual molar ratio of 1:300. Lanes 1 and 4 represent labeled substrates (R11) before addition of the ribozymes. To the substrates was added either the ^{32}P-labeled all-RNA ribozyme (R32, lanes 2 and 3) or the chimeric DRD32 ribozyme (lanes 5 and 6), and the reaction was monitored for 10 min (lanes 2 and 5) and 20 min (lanes 3 and 6) after mixing at 37 °C. After 20 min of incubation, substrates (87 μM) were cleaved almost completely by the chimeric DRD32 ribozyme (>95%, lane 6) whereas about 40% of substrate molecules remained intact when they were treated with the all RNA ribozyme (lane 3). The chimeric DRD32 ribozyme has,

Table 1. Kinetic Parameters[a] and Arrhenius Activation Energies[b] for Ribozyme-Catalyzed Reactions

	k_{cat} (min^{-1})	K_M (μM)	pH-independent limiting k_{cat} (min^{-1})[c]	k_{cat}/K_M (μM^{-1} min^{-1})	$E_{a_{cleav}}$ (kcal mol^{-1})	$E_{a_{diss}}$ (kcal mol^{-1})
R32/R11	4.0	0.02	18	200	16.0[d]	47.7[d]
DRD32/R11	13	1.3	62	10	16.4	39.2

[a] Kinetic parameters (k_{cat}, K_M) were taken from ref 7c. [b] Arrhenius activation energies of chemical cleavage step ($E_{a_{cleav}}$) were calculated at midrange temperatures, 25−50 °C in the case of R32/R11 system and 25−45 °C in the case of DRD32/R11 system. Arrhenius activation energies of dissociation step ($E_{a_{diss}}$) were calculated at temperatures below 25 °C in both systems. [c] The pH-dependent k_{cat} values were measured under saturating conditions, at 37 °C, in the presence of 25 mM $MgCl_2$ and 50 mM Tris-HCl (pH 6.5−9.0) and the pH-independent limiting k_{cat} values were obtained at pH above 9.0. [d] Taken from ref 22.

therefore, higher cleavage activity than the wild-type all-RNA R32 ribozyme.

Kinetic parameters measured at 37 °C, in 25 mM $MgCl_2$ and 50 mM Tris-HCl (pH 8.0), are listed in Table 1 together with the pH-independent limiting k_{cat} values obtained from the pH−rate profile of Figure 4A. Deoxyribonucleotide substitutions at the binding arms increased values of both k_{cat} and K_M. It is to be noted that (i) our DNA-armed ribozyme can cleave more than 10 substrate molecules per minute per ribozyme, and (ii) they do not form any inactive complexes since all the substrate molecules can be cleaved completely. The ability to cleave substrates completely in the present case (Figure 3A, lane 6) differs from the reported abilities of other chimeric ribozymes.[9b]

The k_{cat} Represents the Rate of Cleavage: Thio Effects. Substitution of sulfur for one of the diastereotopic oxygens of a phosphate moiety can be conveniently achieved by automated solid-phase synthesis with standard phosphoramidite building blocks. The effect on the rate of the reaction of the substitution of oxygen by sulfur is commonly referred to as the "thio effect" (i.e., thio effect = $k_{phosphate}/k_{phosphorothioate}$).[28] Recently, studies of the thio effect have frequently been used to probe the rate-limiting step of ribozyme-catalyzed reactions and to identify the coordination site of a metal ion with a phosphate oxygen.[15,19,24,29] In the latter case, the experimental approach relies on the previous measurements of the affinity of divalent ions for ATPβS, since the Mg^{2+} ion is coordinated 30000-fold more strongly to oxygen than to sulfur while the Mn^{2+} ion is coordinated to both oxygen and sulfur more or less equally.[30] Thus, the discrimination by Mn^{2+} ions in binding to either an oxygen or a sulfur atom is poor, while the poor binding of the Mg^{2+} ion to sulfur results in a very large thio effect.[29]

A single phosphorothioate linkage of defined *R*p and *S*p configuration was introduced at the cleavage site of the R11 substrate.[19,24b] The rationale for the experiment is as follows: if a conformational change or the product-release step is the sole rate-limiting step, an alteration of the phosphate at the cleavage site, by introduction of a phosphorothioate linkage, should have very little effect on the overall rate of the reaction (no thio effect would be observed).[15,16] The R11 substrate with either the *R*p or *S*p configuration was incubated either with the all-RNA R32 ribozyme (Figure 3B; lanes 2 and 5) or with the chimeric DRD32 ribozyme (lanes 3 and 6). The amount of 5′ cleavage product clearly indicates that, whereas the *S*p isomer is nearly as reactive as the all-RNA substrate, the *R*p isomer is cleaved only very slowly.

The observed differential thio effect (*S*p vs *R*p) and the metal ion specificity switch (rescue by replacement of Mg^{2+} ions by Mn^{2+} ions; data not shown) appear to indicate that a Mg^{2+} ion is bound directly to the *pro-R* oxygen in both the all-RNA and the chimeric ribozymes. In this arrangement, the bound metal ion can act as an electrophilic catalyst, and thus, the proposed mechanism is very attractive as an explanation of the activities of metalloenzymes.[31] However, more recent, closer examination of the thio effects indicated that Mn^{2+}-mediated cleavage occurs about 20-fold more rapidly than Mg^{2+}-mediated cleavage with *R*p, *S*p, and also with the natural substrate.[24b] Therefore, it seems unlikely that the previously observed "rescue" effects[19] support the proposed direct and specific coordination of a metal ion to the *pro-R*p oxygen in the transition state of a hammerhead ribozyme-catalyzed reaction.[24b] However, recent X-ray analysis of a hammerhead ribozyme identified one potential catalytic metal ion near the *pro-R*p oxygen.[27c] Since the newly captured conformational intermediate appears to demand further conformational change for the following in-line attack, it remains to be answered whether the captured potential catalytic metal ion would stay there in the transition state. Nevertheless, observation of the thio effects and also of rescue effects, for both the all-RNA and the chimeric ribozymes, clearly demonstrates that the k_{cat} values in our ribozyme system represent the rate of the chemical cleavage.

The k_{cat} Represents the Rate of Chemical Cleavage: Slope of Unity in pH−Rate Profiles and Existence of Apparent Solvent Isotope Effects. To distinguish the chemical-cleavage step from the conformational change that precedes the chemical step, the dependence of k_{cat} values on pH (the relationship between pH and the logarithm of the rate; "pH/log rate profile") was examined under the same conditions as those described in the footnote to Table 1, except for the pH. If the cleavage step were the sole rate-limiting step, characteristic properties involving the chemistry would show up in the pH/log rate profile.[25,32] However, if a conformational change prior to the chemical step were the sole rate-limiting step, such a characteristic feature should be absent from the pH/log rate profile. As shown in Figure 4A, the rate [log(k_{cat})] increased linearly with increasing pH with a slope of unity, for both all-RNA[25] and DNA-armed ribozymes. This pH dependency of the ribozyme activity, an indication of a base catalysis, is

(28) Benkovic, S. J.; Schray, K. J. In *The Enzymes*, 3rd ed.; Boyer, P. D., Ed.; Academic Press: New York, 1973; Vol. 8, pp 201−236.

(29) (a) Piccirilli, J. A.; Vyle, J. S.; Caruthers, M. H.; Cech, T. R. *Nature* **1993**, *361*, 85−88. (b) Herschlag, D.; Piccirilli, J. A.; Cech, T. R. *Biochemistry* **1991**, *30*, 4844−4854. (c) Padgett, R. A.; Podar, M.; Boulanger, S. C.; Perlman, P. S. *Science* **1994**, 266, 1685−1688. (d) Podar, M.; Perlman, P. S.; Padgett, R. A. *Mol. Cell Biol.* **1995**, 15, 4466−4478. (e) Michels, W. J.; Pyle, A. M. *Biochemistry* **1995**, *34*, 2965−2977. (f) Sontheimer, E. J.; Sun, S.; Piccirilli, J. A. *Nature* **1997**, *388*, 801−805. (g) Weinstein, L. B.; Jones, B. C. N. M.; Cosstick, R.; Cech, T. R. *Nature* **1997**, *388*, 805−808.

(30) (a) Jaffe, E. K.; Cohn, M. *J. Biol. Chem.* **1979**, *254*, 10839−10845. (b) Pecoraro, V. L.; Hermes, D. J.; Cleland, W. W. *Biochemistry* **1984**, *23*, 5262−5271.

(31) Pyle, A. M. *Science* **1993**, *261*, 709−714.

(32) Dahm, S. C.; Derrick, W. B.; Uhlenbeck, O. C. *Biochemistry* **1993**, *32*, 13040−13045.

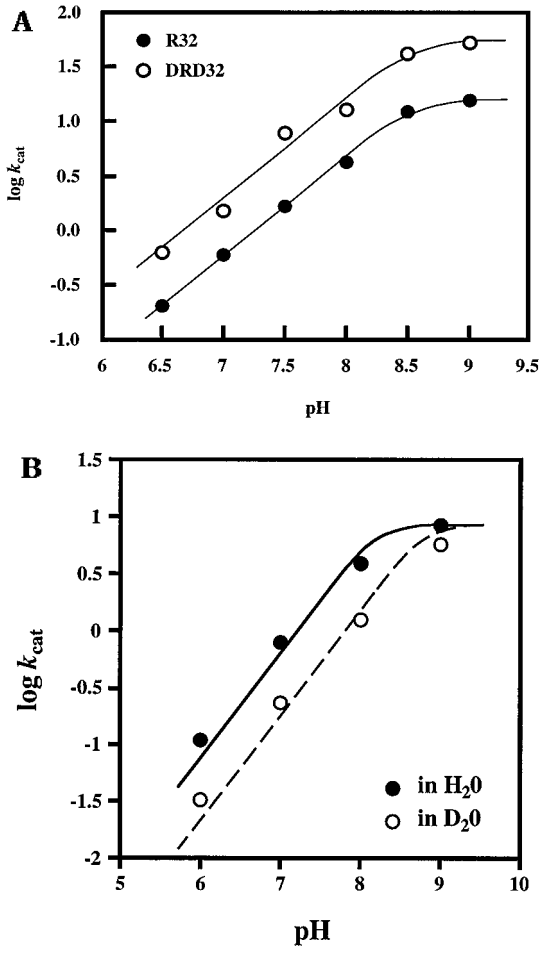

Figure 4. (A) Profiles of pH vs log(k_{cat}). The lower curve with a slope of unity is a theoretical curve calculated on the assumption of a base catalysis with a limiting k_{cat} value of 18 min^{-1} and a pK_a of 8.5, values that fit well with the experimental values for R32 (closed circles). Similarly, the upper theoretical curve with a limiting k_{cat} value of 62 min^{-1} and a pK_a of 8.5 fits with the experimental values for DRD32 (open circles). (B) Profiles of pH vs log(k_{cat}) for the R32 ribozyme-catalyzed reactions, either in H_2O (closed circles) or in D_2O (open circles). The theoretical curve for the reactions in H_2O (solid line) was shifted by 0.64 pH unit to fit the data obtained in D_2O (dotted line). The two sets of experiments were run side by side. The slope of unity between pH 6 and 8 for the R32/R11 and DRD32/R11 combination, apparent deuterium solvent effects, and no burst kinetics at pH 7.0 (ref 7c) clearly indicate that the chemical-cleavage step, rather than a conformational change that precedes the chemical step or the product-dissociation step, is the rate-limiting step.

nearly identical with that reported by Uhlenbeck's group for a hammerhead ribozyme with different binding sequences.[32] The slope of unity in each profile clearly indicates that the k_{cat} in our ribozyme system represents the rate of chemical cleavage step.

The solid curve for the closed circles in Figure 4A with a slope of unity is the theoretical curve calculated on the assumption of general base catalysis with a limiting k_{cat} value of 18 min^{-1} and a pK_a of 8.5 for the general base in the all-RNA ribozyme.[25] Similarly, the data for the DNA-armed ribozyme can be fit with a limiting k_{cat} value of 62 min^{-1} and a pK_a of 8.5. However, similar to the reported results of Dahm et al.,[32] a doubling of the substrate concentration in the plateau region increased the k_{cat} value by ~60%, an indication that the plateau originated from a change of the rate-limiting step and the pK_a of the base is not 8.5: it is larger than 8.5. This interpretation is in accord with the fact that an apparent deuterium solvent isotope effect decreases upon reaching the plateau region (Figure 4B): the rate-limiting step changes from the chemical step to the association step, probably due to deprotonation of uridine and guanosine moieties in the higher pH region. It is to be noted that, if the k_{cat} in our ribozyme system had represented the rate of the conformational change,[27b] we would not have seen the apparent solvent isotope effects in Figure 4B.

The shift of the pH−rate profile in D_2O (apparent solvent isotope effects) can best be explained by the difference in pK_a of the magnesium-bound oxygen in H_2O versus in D_2O.[21,33] Indeed, the estimated pK_a difference (ΔpK_a) for a water molecule coordinated to a Mg^{2+} ion with its p$K_a^{H_2O}$ of 11.4 turned out to be 0.65.[21b] The shift of the theoretical curve for R32-catalyzed reactions in H_2O (closed circles in Figure 4B) by this magnitude (0.65 pH unit) explains well the behavior of the corresponding reactions in D_2O (open circles). In other word, we can estimate the relative concentrations of the active species (Mg^{2+}-OR) in H_2O vs D_2O, as shown in eqs 1 and 2 where M and OR represent metal ion and ribose 2′-oxygen, respectively, assuming that the hydrated metal ions have the same relative ratios of $K_a^{H_2O}/K_a^{D_2O}$ as organic acids.[21,33]

$$M-OH-R \leftrightarrow M-O^{-}-R + H^{+} \quad (1)$$

$$M-OD-R \leftrightarrow M-O^{-}-R + D^{+} \quad (2)$$

The estimation indicated[21] that the concentration of the active species (Mg^{2+}−OR) is about 4 times higher in H_2O than that in D_2O, and thus the rate of the reaction in H_2O is about 4 times faster than that in D_2O, as the result of the perturbation of the pK_a. It can thus be concluded that, in the entire pH region between 6 and 8, the reduction in the level of the active species in D_2O is the sole cause of the lower rate of ribozyme-catalyzed reactions in D_2O (Figure 4B). Thus, the absence of the actual kinetic isotope effects in the step that leads to cleavage of phosphodiester bonds by ribozymes can be interpreted in terms of a mechanism in which proton transfer does not take place during the transition state. This observation is consistent with the double-metal-ion mechanism of catalysis,[21,25,34] in that Mg^{2+} ions are directly coordinated with the attacking and the leaving oxygens (Figure 5). It is to be mentioned, however, that we cannot completely exclude a possibility that a small isotope effect be "buried" inside the pK_a effect. Nevertheless, our recent kinetic analysis, based on R32 ribozyme-mediated cleavage of two kinds of substrate [the parental 5′-oxy substrate (R11 in Figure 1) and the corresponding 5′-thio substrate][24a] demands that we invoke the double-metal-ion mechanism of catalysis for reactions catalyzed by hammerhead ribozymes.[34d]

The k_{cat} Does Not Represent the Rate of Conformational Change at Any Temperatures: Arrhenius Plots. Arrhenius plots were used to detect any changes in rate-limiting steps. Figure 6 shows distinct changes in the slope of the plot for both the all-RNA[22] and DNA-armed ribozymes under multiple-turnover conditions.

(33) (a) Jencks, W. P. In *Catalysis in Chemistry and Enzymology*; McGraw-Hill: New York, 1969; pp 250−253. (b) Bell, R. P.; Kuhn, A. T. *Trans. Faraday Soc.* **1963**, *59*, 1789−1793.

(34) (a) Steitz, T. A.; Steitz, J. A. *Proc. Natl. Acad. Sci. U.S.A.* **1993**, *90*, 6498−6502. (b) Pontius, B. W.; Lott, W. B.; von Hippel, P. H. *Proc. Natl. Acad. Sci. U.S.A.* **1997**, *94*, 2290−2294. (c) Zhou, D.-M.; Taira, K. *Chem. Rev.* **1998**, in press. (d) Zhou, D.-M.; Zhang, L.-H.; Taira, K. *Proc. Natl. Acad. Sci. U.S.A.* **1997**, in press.

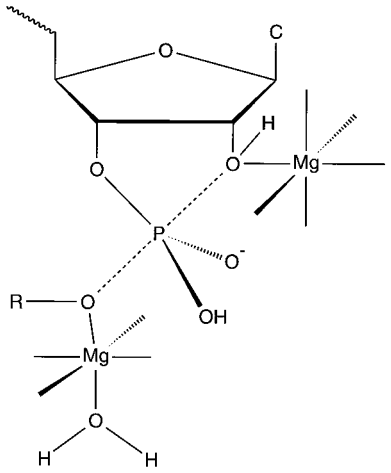

Figure 5. A possible double-metal-ion mechanism of catalysis. The direct coordination of the metal ion with the 2′-oxygen of the attacking nucleotide residue polarizes and weakens the 2′-OH bond. As a result, an inverse correlation between the pK_a of the metal-bound water molecule and the ribozyme activity holds. Similarly, the direct coordination of the metal ion with the 5′-oxygen of the leaving nucleotide residue weakens the 5′-oxygen−phosphorus bond: Metal ions with lower pK_a values will weaken the 5′-oxygen−phosphorus bond to a greater extent and thereby activate the ribozyme-mediated cleavage to a greater extent. In this case, the active species should be completely protonated metal-bound water molecules.

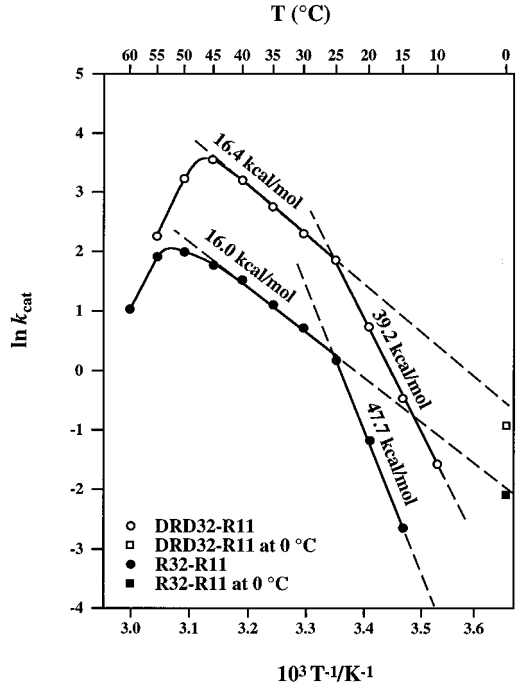

Figure 6. Arrhenius plots for the all-RNA (closed circles) and DNA-armed (open circles) ribozyme-catalyzed reactions. Arrhenius activation energies of R32/R11 combination were calculated to be 16.0 kcal/mol at midrange temperatures (25−50 °C) and 47.7 kcal/mol at lower temperatures (<25 °C) (closed circles) under the substrate saturating conditions, and the corresponding values for the DRD32/R11 combination were 16.4 kcal/mol (25−45 °C) and 39.2 kcal/mol (<25 °C), respectively (open circles). Values obtained under the condition of ribozyme excess (single-turnover condition) at 0 °C for R32/R11 and DRD32/R11 were corresponded to the values extrapolated from the line at midrange temperatures (closed square and open square, respectively).

Since the k_{cat} of DRD32 exceeds 30 min^{-1} at high temperatures, it was not possible to measure kinetics under single-turnover conditions (it was possible only at low temperatures). The plot provides three regions (three different rate-limiting steps in the reaction). In the case of R32 (closed circles in Figure 6), Arrhenius activation energies were calculated to be 16.0 kcal/mol at midrange temperatures (25−50 °C) and 47.7 kcal/mol at lower temperatures (<25 °C). The corresponding values for the DNA-armed DRD32 (open circles) were 16.4 kcal/mol (25−45 °C) and 39.2 kcal/mol (<25 °C). At midrange temperatures, the chemical cleavage step (k_{cleav}) is clearly the rate-limiting step because, as described above, we observed at 37 °C thio effects and rescue effects by Mn^{2+} and because pH−rate profiles and reactions in D_2O also supported this conclusion. The lack of burst kinetics for both R32 and DRD32 at the measurement temperature of 37 °C also supports this conclusion.[7d] Therefore, at midrange temperatures for both R32 and DRD32, (i) the cleaved fragments dissociated from the ribozyme at a higher rate than the rate of the chemical reaction and (ii) any conformational change prior to the cleavage reaction, if such a change had occurred, was also rapid ($k_{cleav} < k_{conf}$, k_{diss}).

When the temperature of the reaction was lowered, at 25 °C a change in the rate-limiting step was recognized. The rate-limiting step at lower temperatures could reflect either a conformational change or it could reflect the product-dissociation step. To distinguish between these two possibilities, k_{cat} was measured at 0 °C under conditions of an excess of ribozyme ([ribozyme] ≫ [substrate]: single-turnover conditions). Under these conditions the product-dissociation step becomes irrelevant. If the rate-limiting step below 25 °C were a conformational change (k_{conf}), required for the formation of the activated complex as suggested by the X-ray data,[26,27] the k_{cat} value at 0 °C should fall on the extrapolated line at temperatures between 25 and 0 °C. By contrast, if the conformational change occurred more rapidly than the chemical cleavage step ($k_{conf} > k_{cleav}$) and if the rate-limiting step below 25 °C were the product-dissociation step, then the observed k_{cat} at 0 °C would fall on the line extrapolated from the region that corresponds to midrange temperatures, 45−25 °C. The observation that the measured k_{cat} values for both R32 and DRD32 under single-turnover conditions at 0 °C fell on the extrapolated lines from the midrange temperatures supports the latter possibility: the rate-limiting step changes upon a decrease in the reaction temperature from the chemical-cleavage step to the product-dissociation step without the involvement of a rate-limiting conformational change. Schematic energy diagrams for these two putative processes for both R32 and DRD32 are shown in Figure 7.

At high temperatures, above 50 °C for R32 and above 45 °C for DRD32, the rate of the reaction decreased, probably because, at such high temperatures, the formation of the Michaelis−Menten complex was hampered by thermal melting (therefore, the rate, k_{obs}, of the reaction at high temperatures does not reflect k_{cat}). The melting temperature (T_m) of stem II of this ribozyme was expected to be around 90 °C.[35] Indeed, the T_m of stem II of this ribozyme was found to be above 80 °C.[23] Therefore, the ribozyme itself is expected to be able to retain its active structure at high temperatures used in this study.

(35) Heus, H. A.; Uhlenbeck, O. C.; Pardi, A. *Nucleic Acids Res.* **1990**, *18*, 1103−1108.

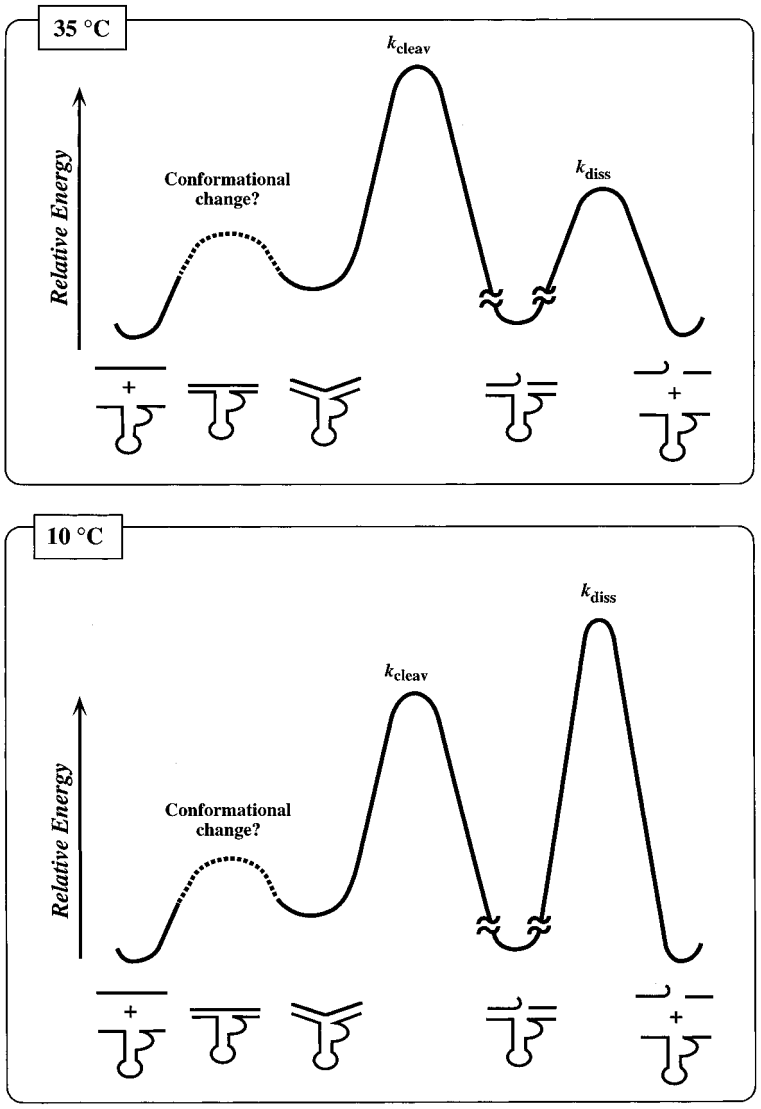

Figure 7. Qualitative energy diagrams for the reaction catalyzed by hammerhead ribozymes. The rate-limiting step changes from the chemical-cleavage step (top) to the product-dissociation step (bottom) at <25 °C without the appearance of a rate-limiting change in conformation.

Table 2. Thermodinamic Parameters for Reactions Catalyzed by All-RNA and DNA-Armed Ribozymes[a]

	10 °C		35 °C	
	R32[b]	DRD32	R32[b]	DRD32
$\Delta G^{\ddagger}$ (kcal/mol)	22.9	21.2	19.9	18.9
$\Delta H^{\ddagger}$ (kcal/mol)	47.1	38.6	15.4	15.8
$\Delta S^{\ddagger}$ (eu)	+85.6	+61.5	−14.6	−10.1

[a] The calculations are based on the transition state theory. Entropy values are given in eu (cal/mol K). [b] Taken from ref 22.

Parameters from the Arrhenius plot were converted to thermodynamic activation parameters by application of transition-state theory.[36] The energy parameters for the multiple-turnover ribozyme-catalyzed reactions at 10 °C, where the dissociation step is the rate-limiting step, and at 35 °C, where the cleavage step is the rate-limiting step, were calculated and are shown in Table 2. (These numbers were reproducible from two independent sets of experiment.) $\Delta H^{\ddagger}$ values, at the reaction temperature of 35 °C, with the cleavage step being the rate-limiting step, were calculated to be 15.4 and 15.8 kcal/mol for R32 and DRD32, respectively. The identical $\Delta H^{\ddagger}$ values for both types of ribozyme indicate that, once the activation complex had formed, the energy required for the chemical cleavage remained unchanged despite the higher reactivity of the DNA-armed ribozyme. By contrast, at lower temperatures, two types of ribozyme yielded different $\Delta H^{\ddagger}$ values. $\Delta H^{\ddagger}$ values, at the reaction temperature of 10 °C, with the dissociation step being the rate-limiting step, were calculated to be 47.1 and 38.6 kcal/mol for R32 and DRD32, respectively. The smaller $\Delta H^{\ddagger}$ value at 10 °C for the DNA-armed ribozyme correlates with the larger K_M value for the DRD32 (note in Table 1 that the DNA-armed ribozyme has about 60-fold higher K_M value compared to that of the all-RNA ribozyme), reflecting the expected poorer stability of DNA/RNA heteroduplex compared to the corresponding RNA/RNA duplex.[12,37]

In agreement with the above assignments for the rate-limiting steps, $\Delta S^{\ddagger}$ at 35 °C is negative for the two types of ribozyme, results that suggest the existence, in the transition state of the chemical cleavage process, of some ordered structure involving, for example, correct positioning of the catalytic Mg^{2+} ion(s), as shown in Figure

(36) Jencks, W. P. In *Catalysis in Chemistry and Enzymology*; McGraw-Hill: New York, 1969; pp 599−614.

(37) Walker, G. T. *Nucleic Acids Res.* **1988**, *16*, 3091−3099.

5. It is of particular interest that $\Delta H^{\ddagger}$ values at 35 °C were identical for the two types of ribozyme and the higher cleavage activity of the DNA-armed ribozyme stems exclusively from the more favorable $\Delta S^{\ddagger}$ (−10.1 eu for DRD32 vs −14.6 eu for R32). As expected, $\Delta S^{\ddagger}$ at 10 °C, at which the product-dissociation step is the rate-limiting step, is positive, reflecting the partial release of the cleavage products from the ribozyme.

It is to be emphasized that, under all the conditions examined, the conformational change did not become the rate-limiting step in our ribozyme system. It is well-known that the tertiary structure of ribozymes is very sensitive to the concentration of Mg^{2+} ions, reflecting the existence of several conformational intermediates.[9cd,38] The observations of a "thio effect", the unit slope in the pH−rate profile, the "apparent" solvent isotope effects and a change of a rate-limiting step, from the chemical cleavage to product dissociation, indicate that the conformational change is rapid in our ribozyme system,[23] and thus the active and inactive conformers are in rapid equilibrium (with respect to the cleavage step).

Structures of Transition States and Active Ribozyme·Substrate Complexes. As part of our efforts at elucidating structure−function relationships we compared the kinetic and thermodynamic features of all-RNA and DNA-armed ribozymes. We found that both R32 and DRD32 should undergo rapid conformational change prior to cleavage from the ground-state structure identified by the X-ray crystallography,[26,27] at all temperatures and in the entire pH region between 6 and 8: no rate-limiting conformational change was found under all the conditions examined. Moreover, DNA-arms enhanced the rate of cleavage (k_{cleav}) as well as the rate of product dissociation (k_{diss}).

Regarding the transition state structure of the ribozyme-catalyzed reaction,[21] as pointed out by von Hippel,[34b] the direct coordination of the metal ion with the 2′-oxygen of the attacking nucleotide residue as shown in Figure 5 polarizes and weakens the 2′-OH bond.[25] As a result, the equilibrium in eq 1 shifts to the right, yielding higher concentrations of active nucleophiles (M−O$^-$−R). Therefore, an inverse correlation between the pK_a of the metal-bound water molecule and the ribozyme activity holds.[32,34b] Similarly, the direct coordination of the metal ion with the 5′-oxygen of the leaving nucleotide residue, as shown in Figure 5, weakens the 5′-oxygen−phosphorus bond:[21,25,39] Metal ions with lower pK_a values will weaken the 5′-oxygen−phosphorus bond to a greater extent, and thereby activate the ribozyme-mediated cleavage to a greater extent.[34b] Indeed, the first experimental evidence of Mg^{2+} ion acting as a Lewis acid catalyst is reported in the case of *Tetrahymena* ribozyme.[29a] Substitution of the 5′-leaving oxygen with a sulfur yields a hammerhead substrate whose leaving group now should be stabilized by soft divalent metal ions relative to the harder Mg^{2+} ion, if the proposed Lewis acid catalyst exists. However, unlike the case of the *Tetrahymena* ribozyme,[29a] no such acceleration in reaction rate was observed,[24a,40] suggesting that the leaving oxygen is not stabilized by a divalent metal ion binding directly to it.[40] However, such metal ion coordination would only have been observed if the cleavage of the P−S bond were rate-limiting.[24a,41] Since we found that the cleavage of the P−S bond was not the rate-limiting step in a reaction catalyzed by a hammerhead ribozyme,[24a] the double-metal-ion mechanism[34a] for the hammerhead ribozyme cannot be rigorously ruled out by the experiments using 5′-sulfur substrate.[34b−d]

If a metal ion acting as a Lewis acid stabilizes the 5′-oxygen as the scissile bond breaks, then the ionic state of the active species should be completely protonated state of metal-bound water molecules (left species in eq 3 where (P)R′O represents the phosphorus-bound 5′-oxygen).

$$(P)R'O-M-OH_2 \leftrightarrow (P)R'O-M-O^-H + H^+ \quad (3)$$

Then, in a pH−rate profile of a ribozyme-catalyzed reaction, one would expect a slope of unity from eq 1 and a slope of −1 from eq 3, resulting in a bell-shaped pH−rate profile. Such bell-shaped pH−rate profiles are common for imidazole-catalyzed hydrolysis of RNA and RNase A catalyzed hydrolysis of RNA, in that the optimum activity can be found around pH 7, reflecting the pK_a of the catalytic molecules (imidazole or histidine).[42] In the case of ribozyme-catalyzed reactions, the activity increases linearly with pH from pH 6 to pH 9, as shown in Figure 4 in accord with eq 1. However, because of the high pK_a of the metal-bound water molecules (>10), the decrease in the activity (eq 3) at even higher pHs is not discernible experimentally.

Recent constrained molecular dynamics (MD) simulations of a hammerhead ribozyme suggested that the double-metal-ion mechanism of catalysis is operative whereby acid/base catalysts are provided from the hydration sphere of the μ-hydroxo-bridged Mg^{2+} ions.[43] Although such a mechanism is attractive, the required proton shuffling within the hydration sphere does not fit with our finding of the absence of solvent isotope effects [after correction of the difference in pK_a (Figure 4B)]. Experimental evidence for the double-metal-ion mechanism of catalysis, in that metal ions are directly coordinated with the attacking and the leaving oxygens (Figure 5), in reactions catalyzed by hammerhead ribozymes will be reported elsewhere.[34d] It is to be emphasized that this mechanism (Figure 5) is identical with the experimentally proven double-metal-ion mechanism of catalysis for the *Tetrahymena* ribozyme.[29g]

Recently, the contribution of several individual ribozyme·substrate base pairs to binding and catalysis was investigated using hammerhead ribozyme substrates that were truncated at their 5′ or 3′ ends.[20b] Addition of residues close to the cleavage site contributed in the chemical step of the hammerhead reaction, but not in the substrate binding step, whereas base pairs distal to

(38) (a) Amiri, K. M. A.; Hagerman, P. J. *Biochemistry* **1994**, *33*, 13172−13177. (b) Amiri, K. M. A.; Hagerman, P. J. *J. Mol. Biol.* **1996**, *261*, 125−134. (c) Bassi, G. S.; Mølledaard, N.-E.; Murchie, A. I. H.; von Kitzing, E.; Lilley, D. M. J. *Nat. Struct. Biol.* **1995**, *2*, 45−55. (d) Bassi, G. S.; Murchie, A. I. H.; Lilley, D. M. J. *RNA* **1996**, *2*, 756−768. (e) Menger, M.; Tuschl, T.; Eckstein, F.; Porschke, D. *Biochemistry* **1996**, *35*, 14710−14716. (f) Simorre, J.-P.; Legault, P.; Hanger, A. B.; Michiels, P.; Pardi, A. *Biochemistry* **1997**, *36*, 518−525.

(39) (a) Taira, K.; Uebayasi, M.; Maeda, H.; Furukawa, K. *Protein Eng.* **1990**, 3, 691−701. (b) Taira, K.; Uchimaru, T.; Storer, J. W.; Yelimiena, A.; Uebayasi, M.; Tanabe, K. *J. Org. Chem.* **1993**, 58, 3009−3017. (c) Uchimaru, T.; Uebayasi, M.; Tanabe, K.; Taira, K. *FASEB J.* **1993**, *7*, 137−142.

(40) (a) Kuimelis, R. G.; McLaughlin, L. W. *J. Am. Chem. Soc.* **1995**, *117*, 11019−11020. (b) Kuimelis, R. G.; McLaughlin, L. W. *Biochemistry* **1996**, *35*, 5308−5317.

(41) Thomson, J. B.; Patel, B. K.; Jiménez, V.; Eckart, K.; Eckstein F. *J. Org. Chem.* **1996**, *61*, 6273−6281.

(42) Anslyn, E.; Breslow, R. *J. Am. Chem. Soc.* **1989**, *111*, 5972−5973.

(43) Hermann, T.; Auffinger, P.; Scott, W. G.; Westhof, E. *Nucleic Acids Res.* **1997**, *25*, 3421−3427.

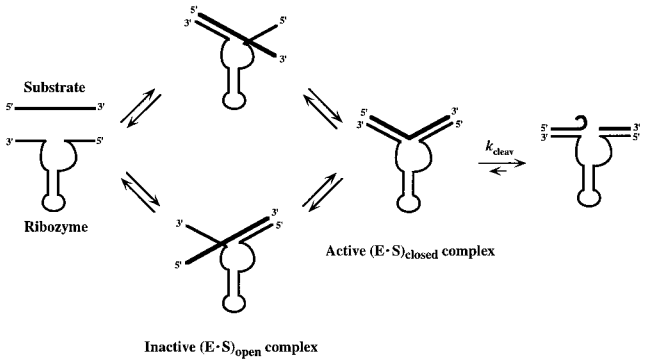

Figure 8. Fraying model with open and closed ribozymesubstrate helixes proposed by Hertel et al.[20b] Each ribozyme·substrate helix can exist in either an unpaired [inactive "$(E\cdot S)_{open}$" complex] state or a helical state [active "$(E\cdot S)_{closed}$" complex], with the closed state required for catalysis. When either helix I (stem I in Figure 1) or helix III (stem III) has sufficiently reduced stability, one or the other of the inactive "$(E\cdot S)_{open}$" complexes will accumulate at equilibrium.

the cleavage site contributed solely to binding but had no effect on the chemical step. These results led to a "fraying model" in which each ribozyme·substrate helix can exist in either an unpaired [inactive "$(E\cdot S)_{open}$" complex in Figure 8] state or a helical state [active "$(E\cdot S)_{closed}$" complex], with the closed state required for catalysis. According to this model, the cleavage rate depends on the concentration of the active $(E\cdot S)_{closed}$ complex relative to that of the inactive $(E\cdot S)_{open}$ complex since both helixes at the binding arms must be formed for the ribozyme to cleave its substrate. This model predicts that, as long as the chemical step is concerned, decreases in cleavage rate should be observed for DNA-armed ribozymes since the DNA·RNA duplexes, which are generally weaker than the corresponding RNA·RNA duplexes as reflected in the 65-fold higher K_M of the DRD32·R11 complex relative to that of the R32·R11 complex (Table 1), fray to give more of inactive $(E\cdot S)_{open}$ complexes.[20b] However, the present study demonstrates that, despite the significantly lower concentration of the active $(DRD32\cdot R11)_{closed}$ complex compared with that of the active $(R32\cdot R11)_{closed}$ complex, the overall activity of the former complex was higher than that of the latter complex (Table 1). This finding argues against the identical and universal structure for the active $(E\cdot S)_{closed}$ complex, for the natural all-RNA and chimeric DNA-armed ribozymes, that leads to the transition state.

We propose that the hybrid helixes of the DNA-armed ribozyme·substrate complex create a slightly different $(E\cdot S)_{closed}$ structure, resulting in a significantly higher activity of the DRD32·R11 complex compared with that of the R32·R11 complex [even so after correction of concentrations of the active $(E\cdot S)_{closed}$ complexes]. It is to be emphasized again that $\Delta H^{\ddagger}$ values for the chemical cleavage step were identical for both all-RNA and DNA-armed ribozymes and the higher cleavage activity of the DNA-armed ribozyme originated exclusively from the more favorable $\Delta S^{\ddagger}$ (-10.1 eu for DRD32 vs -14.6 eu for R32). Exactly the same phenomenon was observed for a similar ribozyme with different length in binding arms (data not shown). Apparently, the DNA-armed ribozyme·substrate complex [the active $(DRD32\cdot R11)_{closed}$ complex] is closer to the transition state structure because of the hybrid helixes, and thus a smaller reorganization (conformational change of a smaller magnitude) will lead to the transition state structure, e.g. such as the one shown in Figure 5.

Acknowledgment. We thank Eric Anslyn at the University of Texas at Austin for helpful comments on the manuscript.

JO9712411